International Conference on Lightning Protection
33rd International Conference on Lightning Protection
25 - 30 September 2016
Estoril, Portugal

Full-Wave Modelling of a Counterpoise

Antonio P.C. Magalhães
COPPE/UFRJ
Universidade Federal do Rio de Janeiro
Rio de Janeiro, RJ, Brasil
apcm@dee.ufrj.br

Antonio C. S. Lima
COPPE/UFRJ
Universidade Federal do Rio de Janeiro
Rio de Janeiro, RJ, Brasil
acsl@dee.ufrj.br

Maria Teresa Correia de Barros
Instituto Superior Técnico
Universidade de Lisboa (UL)
Lisboa, Portugal
teresa.correiadebarros@ist.ulisboa.pt

***Abstract*—This paper proposes a distinct approach for the modeling of a counterpoise. Instead of using either finite or infinite transmission line modeling based on quasi-TEM (transverse electromagnetic) wave propagation, a full-wave modeling of a counterpoise is presented. Initially, it is summarized the development of a full-wave model from the solution of the integral equation to determine to propagation constant, γ. One advantage of the full-wave modeling is related to direct determination of the electromagnetic field in the surrounding media. From the knowledge of γ an equivalent transmission line model is derived. Time-domain responses of the ground potential rise are obtained using the Numerical Laplace Transform.**

Keywords-lightning performance, fullwave modeling, fast transients.

I. INTRODUCTION

A key element in the evaluation of the lightning performance of any transmission circuit is the counterpoise. The technical literature is rather large. The early works relied on the data experimentally available data in the 1930s [1][2] while the first theoretical approaches relied on simplified expressions [3][4]. Since then there has been mainly to approaches for dealing with a counterpoise. The first one assumes that a counterpoise as a finite length transmission line using the so-called cylindrical electrode [5]. The second one relies in analyzing a counterpoise as a transmission line in lossy media [6][7]. In either case, a quasi-TEM (Transverse Electromagnetic) propagation is assumed. However, from a more general approach, a full-wave modeling such as the work proposed by Wait [8] using Hertz vectors or Kikuchi [9] using electric scalar and magnetic vector potentials could be preferable for a general assessment of lightning performance.

In this paper, we propose to use a full-wave model to represent a counterpoise and it is structured as follows. Section II outlines the basics of a full-wave model and how to determine the modal equation used to calculated the propagation constant. This section also presents the expressions for the impedance and admittance per unit length (pul) s well as the ones related to the propagation parameters, i.e. characteristic impedance and propagation function) derived from a full-wave model. In section III, we present some frequency domain results associated with the full-wave formulation of the counterpoise. For these and the following tests we considered three possibilities for representation of the ground parameters, namely, a frequency independent ground model considering both ground conductivity and permittivity and two frequency dependent ground model based on [10][11]. Section IV outlines the time-domain responses based on Numerical Laplace Transformation (NLT) formulation of the problem. The main conclusions of the paper are presented in section V and in Appendix A further details of the full-wave formulation are presented.

This work was supported in part by a funding from INERGE (Instituto Nacional de Engenharia Elétrica) CAPES, CNPq, FAPEMIG, FAPERJ and ERASMUS MUNDUS SMART2.

II. FULL-WAVE MODELLING

As shown in [12], the full-wave model presented here and originally formulated by Wait in [8] leads to the same modal equation as the model proposed by Kikuchi [9]. This model was further improved in [13] to include conductor losses. In Appendix A, we outline how one can connect both approaches. An evaluation of a full-wave model for buried bare and coated conductor in power engineering indicated that the range of application of the quasi-TEM modeling is around 10 MHz [14].

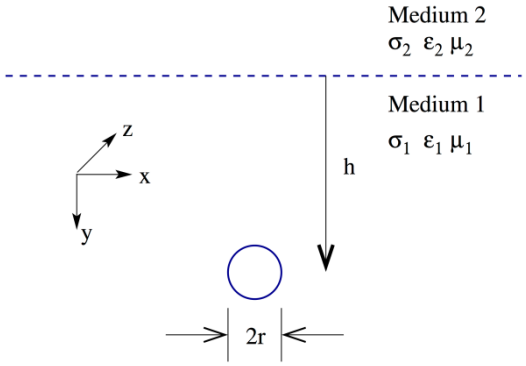

Fig. 1. Conductor configuration

Initially consider a conductor at a constant depth in a lossy medium as depicted in Fig. 1. Assuming an injected current $\mathbf{I} = i_0 \exp(j\omega t)\exp(-\gamma z)$ where γ is an unknown propagation constant to be determined and medium 1 as ground. For a generic point *(x,y,z)* in medium 1, the scalar electric potential is given by

$$\varphi(x,y,z) = \frac{i_o \exp(-\gamma z)}{2\pi} \frac{\gamma}{(\sigma_1 + j\omega\epsilon_1)} \left[\Lambda(x,y) + S_2(x,y)\right] \quad (1)$$

and the components A_y and A_z of the magnetic vector potential are given below, (A_x is null).

$$A_y(x,y,z)=\frac{i_o\exp(-\gamma z)}{2\pi}\frac{\gamma R(x,y)}{j\omega(\sigma_1+j\omega\varepsilon_1)}$$
$$A_z(x,y,z)=\frac{i_o\mu_1\exp(-\gamma z)}{2\pi}\left[\Lambda(x,y)+S_1(x,y)\right] \quad (2)$$

In the above equations $\Lambda(x,y)=K_0(d_1\eta)+K_0(d_2\eta)$, $d_1=\sqrt{x^2+(y-h)^2}$, $d_2=\sqrt{x^2+(h+y)^2}$, $\eta=\sqrt{k_1^2-\gamma^2}$, S_1 and S_2 are the Sommerfeld integrals

$$S_1(x,y)=\int_{-\infty}^{\infty}\frac{\exp\left[-u_1(y+h)\right]\exp(-j\lambda x)}{n^2u_1+u_2}d\lambda$$
$$S_2(x,y)=\int_{-\infty}^{\infty}\frac{\exp\left[-u_1(y+h)\right]\exp(-j\lambda x)}{u_1+u_2}d\lambda \quad (3)$$

where $u_1=\sqrt{\lambda^2+\gamma_1^2-\gamma^2}$, $u_2=\sqrt{\lambda^2+\gamma_2^2-\gamma^2}$ and R is given by

$$R(x,y)=\int_{-\infty}^{\infty}\frac{(u_2-u_1)\left(\exp\left[-u_1(y+h)\right]\exp(-j\lambda x)\right)}{n^2u_1+u_2}d\lambda \quad (4)$$

in (3) and (4) $n=\gamma_2/\gamma_1$ is the reflection index between the two media.

The propagation constant γ can be determined by evaluating the electric field at the conductor coordinates, i.e.

$$\mathbf{E}(r,h,z)=-\nabla\varphi(r,h,z)-j\omega\mathbf{A}(r,h,z). \quad (5)$$

This allows writing the modal equation M shown below

$$M=\frac{2\pi}{j\omega\mu_0}z_{int}+\left(1-\frac{\gamma^2}{\gamma_1^2}\right)\Lambda+\left(S_1-\frac{\gamma^2}{\gamma_1^2}S_2\right)=0 \quad (6)$$

where z_{int} is the conductor internal impedance given by

$$z_{int}=\frac{1}{2\pi r}\left(\frac{j\omega\mu_c}{\sigma_c}\right)^{1/2}\frac{I_0(\gamma_c r)}{I_1(\gamma_c r)} \quad (7)$$

where μ_c and σ_c are the magnetic permeability and conductivity of the conductor respectively, and I_0 and I_1 are modified Bessel functions of the first kind, zero and first order, respectively. $\gamma_c\approx\sqrt{j\omega\mu_c\sigma_c}$ is the propagation constant of the conductor. The equation (6) is an integral equation in γ and its solution demands some care from the numerical point of view, see [15] for details.

A. pul parameters

To define the propagation characteristics we must solve the wave equation

$$\frac{d^2U}{dz^2}=Z\cdot Y\cdot U \qquad \frac{d^2I}{dz^2}=Y\cdot Z\cdot I \quad (8)$$

where I is the counterpoise cable current and U is the wire voltage to ground given by

$$U=-\int_0^h E_y dy=\varphi(r,h,0)-\varphi(0,0,0)+j\omega\int_0^h A_y(r,\xi)d\xi. \quad (9)$$

The pul parameters are then given by

$$Z=z_{int}+z_{ext} \qquad Y=y_{ext} \quad (10)$$

In the evaluation of both Z and Y, only the terms z_{ext} and y_{ext} are dependent on the propagation constant γ, and their expressions are shown below

$$z_{ext}=\frac{j\omega\mu_0}{2\pi}\left[\Lambda+S_1-\left(\frac{\gamma}{\gamma_1}\right)^2(T+S_2)\right]$$
$$y_{ext}=2\pi(\sigma_1+j\omega\varepsilon_1)\left[\Lambda-T\right]^{-1} \quad (11)$$

being

$$T=\int_{-\infty}^{\infty}\frac{u_2}{u_1}\frac{\left[\exp(-hu_1)-\exp(-2hu_1)\right]}{n^2u_1+u_2}\exp(-jr\lambda)d\lambda.$$

It is worth mentioning that these expressions are slightly more complex than those proposed by Sunde [16] as in this reference only Hertz vector of electric type were considered.

B. modeling of a counterpoise

Consider the counterpoise shown in Fig.~2 where d is 6 m and L 90 m. In this configuration, the counterpoise will present two modes, one additive and one subtractive. In terms of the actual voltage rise of the tower footing the main interest lies in the additive mode as it is the mode responsible for a current injection in the soil. As a result, we ended up with an equivalent counterpoise given by a single electrode. Furthermore, in practical configurations each conductor has a distance at least one order the magnitude higher than its radius enforcing the idea that a suitable single conductor might be acceptable. However, future work is needed to evaluate whether this assumption is sufficient and if there are some other conditions that should be met to keep this approximation.

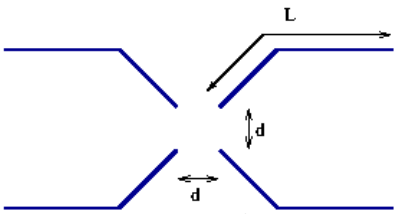

Fig. 2. Counterpoise configuration.

From the full-wave model of the buried cable, a single-phase frequency dependent transmission line will model each counterpoise. Thus, the characteristic impedance, $\mathbf{Y}_c$, the characteristic impedance $\mathbf{Z}_c$ and the propagation function $\mathbf{H}$ can be defined as follows

$$\mathbf{H}=\exp\left(-\ell\sqrt{Y\cdot Z}\right) \qquad \mathbf{Y}_c=\sqrt{Y/Z} \qquad \mathbf{Z}_c=1/\mathbf{Y}_c$$

where ℓ is the length of the counterpoise, Z and Y are defined in the previous section.

Each counterpoise can be assembled as a single-phase line following the structure below

$$\begin{bmatrix}\mathbf{I}_{in}\\0\end{bmatrix}=\begin{bmatrix}\mathbf{Y}_c\cdot\mathbf{A} & -2\mathbf{Y}_c\cdot\mathbf{B}\\ -2\mathbf{Y}_c\cdot\mathbf{B} & \mathbf{Y}_c\cdot\mathbf{A}\end{bmatrix}\begin{bmatrix}\mathbf{V}_{GR}\\\mathbf{V}_f\end{bmatrix} \quad (12)$$

with $\mathbf{A}=\left(1+\mathbf{H}^2\right)\left(1-\mathbf{H}^2\right)^{-1}$, $\mathbf{B}=\mathbf{H}\cdot\left(1-\mathbf{H}^2\right)^{-1}$ and $\mathbf{I}_{in}$ is the injected current, $\mathbf{V}_{GR}$ is the ground voltage rise and $\mathbf{V}_f$ is the

voltage at the end of the counterpoise which is obtained by solving (12) which leads to (13), thus the voltage rise at the counterpoise sending end depends on both the characteristic impedance and the propagation function.

$$\begin{bmatrix} \mathbf{V}_{GR} \\ \mathbf{V}_f \end{bmatrix} = \mathbf{I}_{in} \begin{bmatrix} \mathbf{Z}_c \cdot \left(1+\mathbf{H}^2\right) \cdot \left(1-\mathbf{H}^2\right)^{-1} \\ 2\mathbf{Z}_c \cdot \mathbf{H} \cdot \left(1-\mathbf{H}^2\right)^{-1} \end{bmatrix} \tag{13}$$

For the time-domain responses the Numerical Laplace Transform (NLT) was used in the solution [17][18]. This implied in solving the integral equation several times with is a rather time-consuming task. Improvements on the numerical evaluation might be gained if rational approximation of both $\mathbf{Y}_c$ and $\mathbf{H}$ are considered. This approach was used in [19] for full-wave modeling of an insulated cable. Application of such approach to a full-wave modeling of a counterpoise is left to future work.

III. Frequency Domain Analysis

Consider a counterpoise of length 90m buried at a depth h=0.8m, with radius $r_c = 3.9894 \cdot 10^{-3}$ m. Three possible soil configurations were considered. The first one is a frequency independent soil model with $\sigma_s = 10^{-3}$ S/m and $\epsilon_{rs} = 10.0$ thus considering ground displacement currents. The second soil model is based in [10] which leads to the following ground propagation constant, γ_1 (ground is medium 1 in the present formulation)

$$\gamma_1 = \sqrt{\mathrm{j}\omega\mu\left(\sigma_0 + \Delta_1\left(\frac{\omega}{2\pi \cdot 10^6}\right)^{\alpha_i}\left(\cot\left[\frac{\pi}{2}\alpha_i\right] + j\right)\right)} \tag{14}$$

where σ_0 S/m is the low frequency ground conductivity, and for the sake of comparison assumed to be $\sigma_0 = \sigma_s$, $\Delta_1 = 11.71$ and $\alpha_i = 0.706$. Third soil model considered was proposed in [11], and γ_1 has the following expression

$$\gamma_1 = \sqrt{\mathrm{j}\omega\mu\left(\sigma_s + \mathrm{j}\omega\varepsilon_{rs}\varepsilon_0\right)} \tag{15}$$

where

$$\sigma_s = \sigma_0\left(\frac{\omega}{2\pi \cdot 100}\right)^{0.072} \qquad \varepsilon_{rs} = 2.34 \cdot 10^6\left(\frac{1}{\sigma_0}\right)^{-0.535}\left(\frac{\omega}{2\pi}\right)^{-0.597}$$

and σ_0 is the same as before. Figures 3 and 4 depicts the behavior of the magnitude of the impedance and admittance pul for such counterpoise. Both parameters are rather smooth functions of frequency, however as the magnitude of the impedance was rather similar regardless of the soil model used, the same cannot be said about the admittance which presented a very distinct behavior as a function of the soil model considered. In this and in the following figures the label Conventional stands for the frequency independent model using σ_s and ϵ_{rs} as shown above, Portela stands for the model based on (14) and Visacro is based on (15).

The behavior of Y affects considerably the characteristic impedance, $\mathbf{Z}_c$, and admittance $\mathbf{Y}_c$ as shown in Fig. 5 and 6 respectively. Unlike $\mathbf{Y}_c$, the propagation function $\mathbf{H}$ presented a very similar behavior for all three soil models considered as it can be seen in Fig. 7.

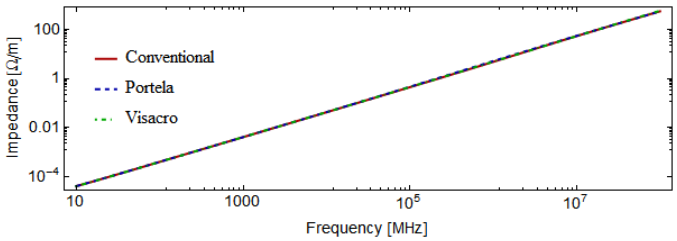

Fig. 3. Magnitude of the impedance per unit length.

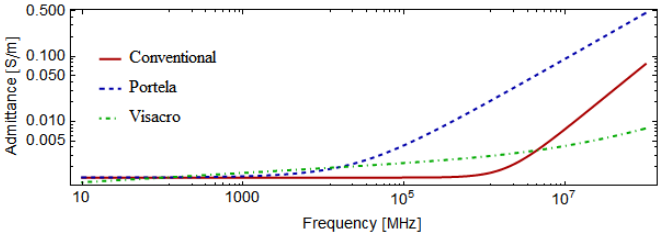

Fig. 4. Magnitude of the admittance per unit length.

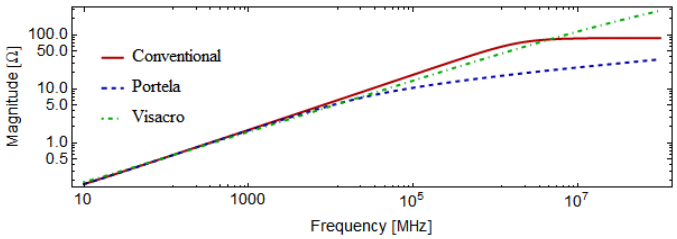

Fig. 5. Magnitude of Characteristic Impedance

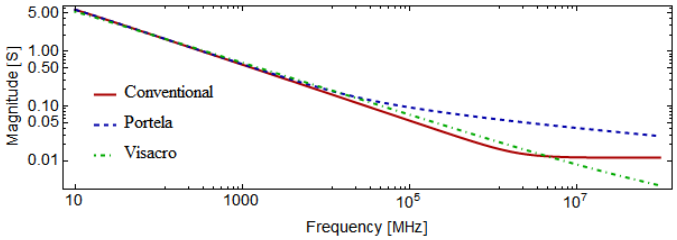

Fig. 6. Magnitude of Characteristic Admittance

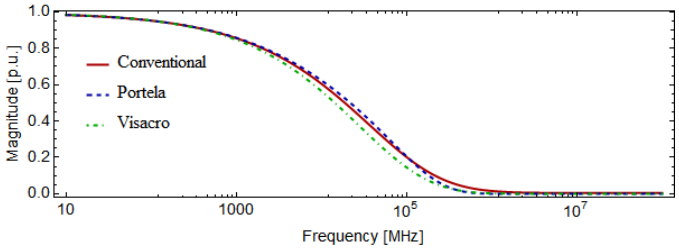

Fig. 7. Magnitude of Propagation Function

One interesting application of using a full-wave model is related to the ability to evaluate the electric and magnetic field associated with the counterpoise for a wide frequency range.

To illustrate this aspect consider a case where the injected current is a unit step. Figure 8 depicts the absolute value of the electric field for the same counterpoise as before but considering different burial depths. The value of the electric field as calculated as $|\mathbf{E}| = \sqrt{|E_x|^2 + |E_y|^2 + |E_z|^2}$. The field is evaluated at coordinates $(0, h, 0)$. It can be noticed that all three models provide similar results up to 100 kHz. The conventional approach gave a similar response to the model based on (15), while the Portela's model had a higher damping. As the counterpoise presented a higher burial depth, the high frequency behavior of the electric field tends to a constant value. It is important to mention that the experimental data used to develop both frequency dependent models is valid only up to 2 MHz.

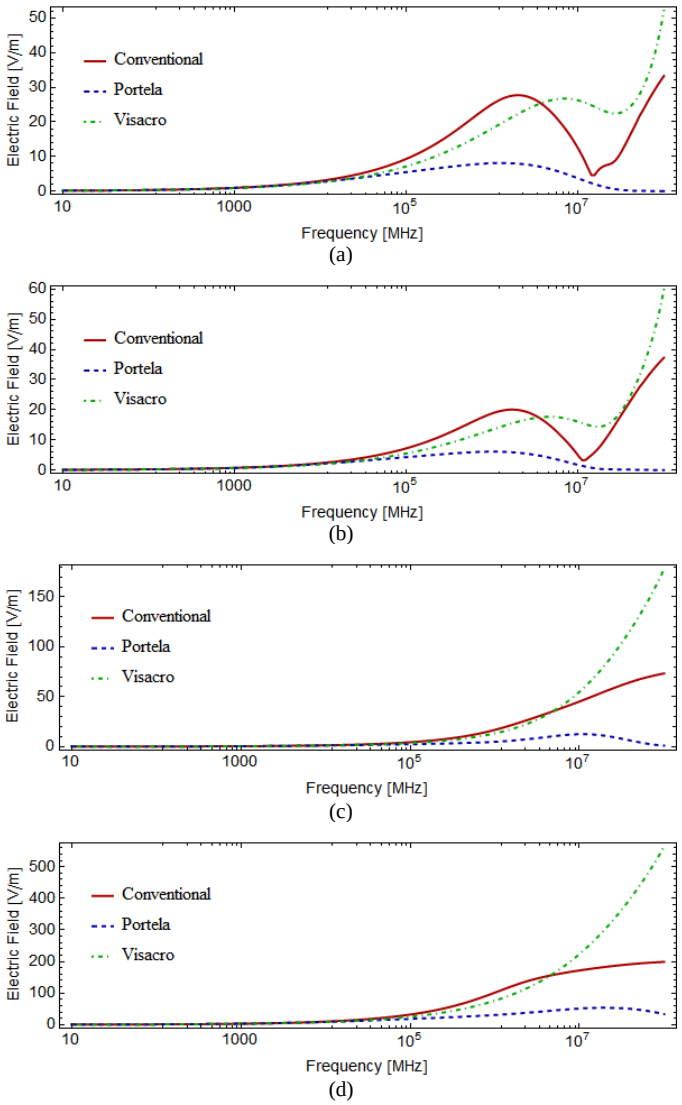

Fig. 8. Frequency Response of Electric Field considering distinct depths: a) h=0.01m, b) h=0.1m, c) h=0.5m and d) h=0.7m.

IV. Time Domain Response

For the analysis of the time-domain response we consider an injection of an impulse current at the sending-end of the counterpoise modeled as a Heidler function, i.e.

$$\mathbf{I}_{in} = \frac{I_{\max}}{\eta}\left(1+\left(\frac{t}{\tau_1}\right)^n\right)e^{\frac{-t}{\tau_2}} \qquad (16)$$

where $I_{max} = 1.0$, $\eta = \left(\frac{t}{\tau_1}\right)^n e^{-\frac{\tau_1}{\tau_2}\left(\frac{n\tau_2}{\tau_1}\right)^{1/n}}$, n=2, τ_1=1.8 μs is the rising time and τ_2=95 μs , decreasing time. The total length of the counterpoise and it is radius are the same as in the previous section. The NLT was used considering 2048 frequency points. The Hanning filter was applied to avoid aliasing the frequency samples. A total simulation time of 40 μs was considered.

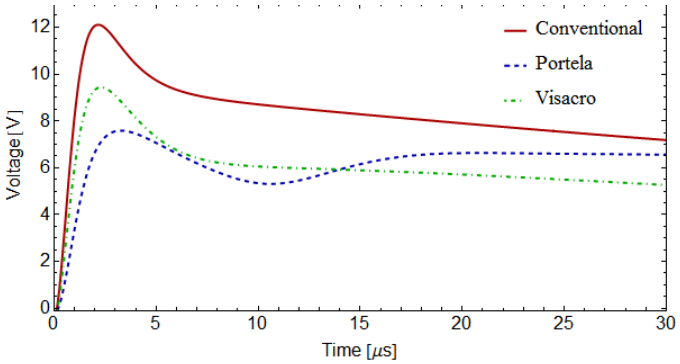

Fig. 9. Ground Voltage rise at the sending ending of the counterpoise due to impulse current injection.

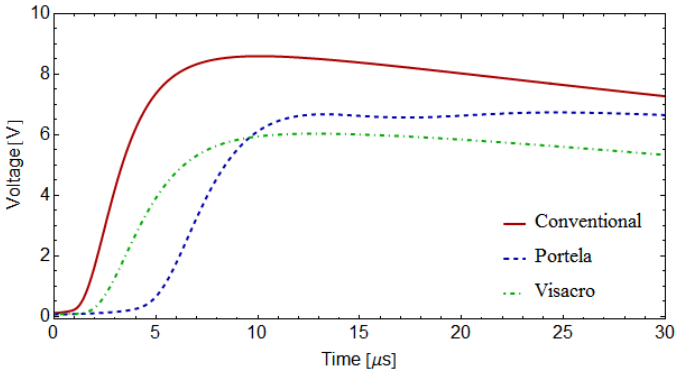

Fig. 10. Voltage rise at the sending ending of the counterpoise due to impulse current injection.

The ground voltage rise $\mathbf{V}_{GR}$ is shown in Fig. 9 below considering the three types of soil modeling. It is interesting to note the conventional soil modeling provide far more steep responses than the ones found with frequency dependent ground parameters. While the asymptotic value of the results using frequency dependent soil models is rather similar, the highest values are considerably different. In the case of the voltage at the sending end of the counterpoise, $\mathbf{V}_f$ see Fig. 10, it is noticed that both frequency dependent soil models provide similar results with respect to maxima. All three models provide different values for the tail response. The effect of the

inclusion of the frequency dependent soil model seems to affect considerably the voltage rise time at the sending end.

V. CONLUSIONS

The work focused on applying a full-wave modeling of a counterpoise. The main advantage of this approach is to assess the behavior of the voltage and current at the counterpoise as well as the electromagnetic field in the surrounding media without the limitation associated with the quasi-TEM approximation. The main drawback of a full-wave model is the need to solve an integral equation for every frequency to determine the behavior of the propagation constant. This procedure is very time-consuming. This presents a challenge for a more efficient simulation in the frequency domain as used in this paper. Numerical improvements might be obtained if rational approximation are used in the fitting of the propagation functions involved.

The evaluation of the propagation functions considered three type of soil model. The results showed that the main differences lies in behavior of the characteristic impedance (or admittance) throughout the frequency range. One advantage of the full-wave model is its ability to include the effect of the displacement current in the ground, which are important in the high frequency range, above hundreds of kHz.

The time-domain responses obtained showed that the asymptotic behavior of the three soil models were similar although noticeable differences appeared. As expected, the frequency dependent soil models presented a higher damping when compared with frequency independent soil model.

Future work is needed to assess the behavior of a more realistic counterpoise configuration when the mutual coupling between counterpoises is considered.

There is a need to obtain soil models suitable for frequencies up to a few tenths of MHz to assess the behavior of the modeling in the high frequency range.

APPENDIX A – FULL-WAVE FORMULATION

For this formulation, we consider two semi-infinite media respectively named "1" and "2" as depicted in Fig 1. In medium "1" there is a counterpoise conductor where the injected current has the form $I = I_{\max} \exp(-\gamma z + j\omega t)$ where γ is the unknown propagation constant to be determined. The electric and magnetic field in both media can be expressed by two Hertz Vectors, one of the electric type, $\mathbf{\Pi}_E$ and other of the magnetic type, $\mathbf{\Pi}_M$. So the fields in media *i* are given from

$$\begin{aligned} \mathbf{E}_i &= \nabla\times\nabla\times\mathbf{\Pi}_{E_i} - j\omega\mu_i\nabla\times\mathbf{\Pi}_{M_i} \\ \mathbf{H}_i &= (\sigma_i + j\omega\varepsilon_i)\nabla\times\mathbf{\Pi}_{E_i} + \nabla\times\nabla\times\mathbf{\Pi}_{M_i} \end{aligned} \quad (A.1)$$

Both Hertz vectors have a single component in the direction of propagation and its relation with vector potential in media *i*, $\mathbf{A}_i$, and electric scalar potential φ_i can be obtained by

$$\mathbf{A}_i = \mu(\sigma + j\omega\varepsilon)\mathbf{\Pi}_{E_i} + \mu\nabla\times\mathbf{\Pi}_{M_i}\ ,\ \varphi_i = -\nabla.\mathbf{\Pi}_{E_i} \quad (A.2)$$

Assuming the continuity of tangential components of $\mathbf{E}_i$ and $\mathbf{H}_i$ is possible to obtain an expression for the electric field in both media. In the first works on the matter [8][9], the modal equation is found considering the electric field null at the surface of the conductor but the inclusion of conductor losses is straightforward, see [13].

REFERENCES

[1] O. Brune, J. Eaton, J.R., "Experimental Studies in the Propagation of Lightning Surges on Transmission Lines," *Trans. American Institute of Electrical Engineers*, vol.50, no.3, pp.1132-1138, Sept. 1931

[2] P. Sporn, "Lightning Experience on 132 kV Transmission Lines of the American Gas and Electric Company System 1930-1931," *Trans. American Institute of Electrical Engineers*, vol.52, no.2, pp.482-490, June 1933

[3] L. Bewley, "Theory and Tests of the Counterpoise," *Trans. American Institute of Electrical Engineers*, vol.53, no.8, pp.1163-1172, Aug. 1934

[4] C. Fortescue, "Counterpoises for Transmission Lines," *Trans. American Institute of Electrical Engineers*, vol.53, no.12, pp.1781-1790, Dec. 1934

[5] J. Salari Filho and C. Portela, "A methodology for electromagnetic transients calculation –an application for the calculation of lightning propagation in transmission lines," *IEEE Trans. on Power Delivery*, vol. 22, no. 01, pp. 527–536, Jan. 2007

[6] Mazzetti, C., and Veca, G.M.: 'Impulse behaviour of grounding electrodes', *IEEE Trans. Power Appar. Syst.*, 1983, PAS-102, (9), pp. 3148–3156

[7] M. Lorentzou, N. Hatziargyriou, and B. Papadias, "Time domain analysis of grounding electrodes impulse response," *IEEE Trans. Power Deliv.*, 2003, PWRD-18, (2), pp. 517–524

[8] J. Wait, "Theory of wave propagation along a thin wire parallel to an interface," *Radio Sci.*, vol. 7, pp. 675-679, June 1972.

[9] H. Kikuchi, "Wave propagation along an infinite wire above ground at high frequencies," *Eletrotech. J. Japan*, vol. 2, pp. 73–78, 1956.

[10] C. M. Portela, "*Measurement and modeling of soil electromagnetic behavior*," in Proc. IEEE Int. Symp. Electromagn. Compat, 1999, vol. 2, pp. 1004–1009.

[11] S. Visacro and R. Alipio, "Frequency dependence of soil parameters: Experimental results, predicting formula and influence on the lightning response of grounding electrodes," *IEEE Transactions on Power Delivery*, vol. 27, no. 2, pp. 927–935, Apr. 2012.

[12] P. Pettersson, "Propagation of waves on a wire above a lossy ground-different formulations with approximations," *IEEE Trans. on Power Delivery*, vol. 14, no. 3, pp. 1173-1180, 1999.

[13] M. D'Amore, M. Sarto, "Simulation models of a dissipative transmission line above a lossy ground for a wide-frequency range. I: single conductor configuration," *IEEE Trans. on Electromagnetic Compatibility*, vol. 38, no. 2, pp. 127-138, 1996.

[14] A. P. C. Magalhães, J. C. L. V. Silva, A. C. S. Lima, and M. T. Correira de Barros, "Validation limits of quasi-TEM approximation for buried bare and insulated cables," *IEEE Trans. Electromagnetic Compatibility*, vol. 57, Issue 6, pp. 1690-1697, Dec 2015. DOI: 10.1109/TEMC.2015.2489461

[15] A. C. S. Lima, M. Yanque Tomasevich, "Numerical Issues in Line Models Based on a Thin Wire Above a Lossy Ground," *IEEE Transactions on Electromagnetic Compatibility*, vol.57, no.3, pp.555-564, June 2015.

[16] E. Sunde, *Earth Conduction effects in transmission systems*, 2nd ed, New York: Dover, 1968.

[17] L. Wedepohl and S. E. T. Mohamed, "Multiconductor transmission lines. theory of natural modes and Fourier integral applied to transient analysis," *Proceedings of the Institution of Electrical Engineers*, vol. 116, no. 9, pp. 1553–1563, 1969.

[18] P. Gomez and F. A. Uribe, “The numerical Laplace transform: An accurate technique for analyzing electromagnetic transients on power system devices,” *International Journal of Electrical Power & Energy Systems*, vol. 31, no. 2-3, pp. 116–123, 2009.

[19] A. P. C. Magalhães, A. C. S. Lima, and M. T. Correira de Barros, “Rational Approximation to Full-Wave Modeling of Underground Cables*” In: IPST’15 – International Conference on Power Systems Transients*, Cavtat, Croatia, June 2015. [Online]. Avaliable: http://www.ipst2015.com/openconf/modules/request.php?module=oc_proceedings&action=summary.php&id=69&a=Accept